



UDC 537.9

EDN VYWZTC

<https://www.doi.org/10.33910/2687-153X-2024-5-2-91-103>

As₄Se₄ crystal versus As₄Se₄ molecule: A plane wave DFT study of the geometric and electronic structure

A. A. Gavrikov ^{✉1}, V. G. Kuznetsov ², V. A. Trepakov ²

¹ Herzen State Pedagogical University of Russia, 48 Moika Emb., Saint Petersburg 191186, Russia

² Ioffe Institute, 26 Polytekhnicheskaya Str., Saint Petersburg 194021, Russia

Authors

Anton A. Gavrikov, ORCID: 0000-0001-6121-2013, e-mail: agavrikov@herzen.spb.ru

Vladimir G. Kuznetsov, ORCID: 0000-0003-1996-0055, e-mail: vladimir.kuznetsov@mail.ioffe.ru

Vladimir A. Trepakov, e-mail: trevl@mail.ioffe.ru

For citation: Gavrikov, A. A., Kuznetsov, V. G., Trepakov, V. A. (2024) As₄Se₄ crystal versus As₄Se₄ molecule: A plane wave DFT study of the geometric and electronic structure. *Physics of Complex Systems*, 5 (2), 91–103. <https://www.doi.org/10.33910/2687-153X-2024-5-2-91-103> EDN VYWZTC

Received 4 March 2024; reviewed 11 April 2024; accepted 11 April 2024.

Funding: This study was partly supported by the Ministry of Education of the Russian Federation as part of the state-commissioned assignment (project No. VRFY-2023-0005).

Copyright: © A. A. Gavrikov, V. G. Kuznetsov, V. A. Trepakov (2024) Published by Herzen State Pedagogical University of Russia. Open access under [CC BY-NC License 4.0](https://creativecommons.org/licenses/by-nc/4.0/).

Abstract. Chalcogenide crystals reveal a wide range of changes in chemical and physical properties under band gap light illumination. A majority of these properties are determined by the electronic structure. However, to date there are only a few theoretical articles on the electronic structure of the As₄Se₄ molecule and only two on the As₄Se₄ crystal. We have studied, for the first time, the geometric and electronic structure of the As₄Se₄ crystal versus the As₄Se₄ molecule in the framework of a periodic model by the DFT method within the same approximations. Equilibrium bond lengths and bond angles were calculated together with charge density differences, Mulliken, Löwdin and Bader charges, and also Mulliken overlap populations, and were compared for the crystal and the molecule. A character of chemical bonding in the As₄Se₄ crystal versus the As₄Se₄ molecule was analyzed. The bandstructure DFT calculations were carried out and demonstrated that the As₄Se₄ crystal is an indirect-gap semiconductor.

Keywords: chalcogenides, geometric and electronic structure, chemical bonding, As₄Se₄, molecule, molecular crystal, DFT method

Introduction

Amorphous chalcogenide materials which represent alloys of S or Se with such metals as As, Ge etc. reveal a wide range of changes in chemical and physical properties under band gap light illumination (Elliott 1986; Kolobov 2003; Kolobov, Elliott 1995; Owen et al. 1985). These changes can be reversible or irreversible. While photoinduced structural changes in chalcogenide glasses have been studied intensively since 1980s (Shimakawa et al. 1998; Tanaka 2001; Yang et al. 1987), the electronic structure of molecular chalcogenide crystals together with the photoinduced transition mechanisms have remained deficiently explored. For example, in the As₄Se₄ molecular crystal transition from a crystalline to an amorphous phase can be induced by band gap light (Kolobov, Elliott 1995), and this transition may be reversible. In paper (Krecmer et al. 1997) the another reversible effect, namely so-called the optomechanical effect with the reversible optical-induced optical anisotropy (dichroism), was observed in amorphous As₅₀Se₅₀ thin films. Following the paper (Krecmer, Moulin, Stephenson et al. 1997) upon irradiation with polarized light, thin films of amorphous As₅₀Se₅₀, exhibit reversible nanocontraction parallel to the direction of the electric vector of the polarized light and nanodilatation along the axis orthogonal to the electric vector of the light.

As opposed to amorphous As₄Se₄ there are few studies regarding the crystalline structure of As₄Se₄. The first experimental studies of the As₄Se₄ molecular crystal geometry were performed in 1970s (Bastow, Whitfield 1973; Goldstein, Paton 1974; Renninger, Averbach 1973; Smail, Sheldrick 1974). Realgar-like molecular crystal As₄Se₄ with space group symmetry (P 1 21/c 1) belongs to the monoclinic crystal system and has a unit cell with parameters $a = 9.63 \text{ \AA}$; $b = 13.8 \text{ \AA}$; $c = 6.73 \text{ \AA}$; $\alpha = \gamma = 90^\circ$; $\beta = 107.8^\circ$ (Bastow, Whitfield 1973) consisting of 4 formula units As₄Se₄ as building blocks. As follows from X-ray diffraction studies (Goldstein, Paton 1974), As₄Se₄ is a molecular crystal in which individual As₄Se₄ molecules can be distinguished, having two intramolecular homopolar covalent As–As bonds with slightly different bond lengths of 2.571 Å and 2.560 Å respectively. For comparison, the As–As bond length in amorphous arsenic (a-As) is 2.49 Å (Elliott 1990). The As–As–Se angle, which has its vertex at one of the As atoms that are part of the As–As bonds (101.2° (Goldstein, Paton 1974)), is also significantly larger than the average bond angle of 98° in a-As (Elliott 1990).

The first attempts of theoretical study into the electronic structure of an As₄Se₄ molecular crystal with the unit cell containing four As₄Se₄ molecules used a simplified approach based on a study of the electronic structure of an individual As₄Se₄ molecule by different semi-empirical methods (Chen 1975; Salaneck et al. 1975; Tanaka et al. 1978). Based on the results of these molecular calculations, the photoemission spectra of the crystal were interpreted (Chen 1975; Salaneck et al. 1975). In the first paper (Salaneck et al. 1975) authors used a semi-empirical variant of the self-consistent field method, namely the so-called complete-neglect-of-differential-overlap (CNDO) method; in the second one (Tanaka et al. 1978) — an intermediate-neglect-of-differential-overlap (INDO) method; and in the third one (Chen 1975) — an extended Huckel or Wolfsberg–Helmholz method. Later the calculations of the electronic structure of an individual molecule were already performed using ab initio methods: self-consistent-field $X\alpha$ scattered-wave method (Babić, Rabii 1988) and the density functional method (Babić et al. 1989).

A study of the electronic structure of an individual As₄Se₄ molecule instead of that of a molecular crystal As₄Se₄ is possibly a rough approximation. However, the direct calculation of an As₄Se₄ crystal has long been difficult, especially by ab initio methods, due to the large unit cell of the crystal containing 32 atoms. Therefore, as far as we know no first-principles electronic structure calculations were performed until 1976. The first nonempirical calculation of the electronic structure of pristine crystal As₄Se₄ was accomplished within the chemical pseudopotential approach (Anderson 1969) by the local orbital method (Bullett 1976a) proposed in (Bullett 1975; 1976b). In addition, we know only one more article with the electronic structure ab initio study of the As₄Se₄ crystal (Hasan et al. 2019). In this work the equilibrium geometry of the As₄Se₄ crystal was calculated using the DFT method within Generalized Gradient Approximation (GGA) with the exchange-correlation (XC) functional of PBE (Perdew et al. 1996) type with the help of the plane-wave pseudopotential code VASP. The results of the paper (Hasan et al. 2019) are unsatisfactory, in our opinion, since the parameters of the calculated equilibrium geometry differ significantly from the experimental ones, some by more than 10%. Unsatisfactory results of the unique article with the DFT study of the crystalline As₄Se₄ electronic structure (Hasan 2021; Hasan et al. 2019) were the motivation to accomplish new research.

Methods and computational details

A distinctive feature of molecular crystals is that their potential energy surface (PES) usually has a relatively flat landscape with relatively small local minima, which makes it difficult to optimize geometry and to find the equilibrium geometry (Beran 2016). This problem also occurs for the As₄Se₄ molecular crystal. In this regard, it is of interest to find the theoretical equilibrium geometry of a given crystal and to study a question to what extent the quality of the resulting geometry depends on the methods and approximations used in the calculations.

We studied the dependence of the theoretical equilibrium geometry of the As₄Se₄ crystal calculated by the DFT method against the type of XC functionals and pseudopotentials. To this end, we carried out a series of calculations to fully optimize the geometry of the As₄Se₄ crystal, including lattice parameters and atomic positions, using two plane-wave pseudopotential codes: CASTEP (Clark et al. 2005; Segall et al. 2002) and Quantum Espresso (QE) (Giannozzi et al. 2009; 2017) with GGA XC functionals in the forms of PBE (Perdew et al. 1996) and PBEsol (Perdew et al. 2008), taking into account the van der Waals (vdW) correction in the form of Grimme-D2 (Grimme 2006). To describe

electronic–ionic interactions, two types of pseudopotentials were used, namely the Projector Augmented–Wave (PAW) (Blöchl 1994; Kresse, Joubert 1999) potentials in QE code and the optimized norm-conserving Vanderbilt (ONCV) pseudopotentials (Hamman 2013) in CASTEP and QE codes. The PAW potentials were taken from the PAW data-set generated by Dal Corso (Dal Corso 2014); the ONCV scalar-relativistic pseudopotentials — from the Schlipf–Gygi pseudopotentials library (Schlipf, Gygi 2015) (issue 2020-02-06) for CASTEP code and from PseudoDojo pseudopotentials library (van Setten et al. 2018) for QE code.

The geometry optimization in both codes was performed using the Broyden–Fletcher–Goldfarb–Shanno (BFGS) (Eyert 1996; Pfrommer et al. 1997; Press et al. 1992; Shanno 1978) algorithm. The atomic positions and cell parameters were optimized until the energy difference, the Hellmann–Feynman forces on the atoms, and all the stress components did not exceed the values 1×10^{-7} eV atom⁻¹, 5×10^{-4} eV Å⁻¹, 1×10^{-3} GPa for CASTEP code and the values 1×10^{-8} Ry, 4×10^{-5} Ry bohr⁻¹, 1×10^{-2} kbar for QE code, respectively. It is worth noting here that in QE code it is accepted to use as the energy tolerances the extensive quantities, as opposed to CASTEP code. The convergence criteria of a self-consistent energy process were specified by the tolerance values 1×10^{-8} eV atom⁻¹ for CASTEP code and 1×10^{-10} Ry for QE code.

The convergence of total energy with respect to the density of the Monkhorst–Pack k-mesh (Monkhorst, Pack 1976) in the irreducible Brillouin zone (IBZ) and to the plane-wave kinetic energy cutoff was studied. It was found that to achieve the convergence of total energy within a few meV the following values of the energy cutoff should be taken: 1200 eV for the ONCV pseudopotentials in code CASTEP and 98 Ry for ONCV pseudopotentials and PAW potentials in code QE. For given cutoff energies, convergence of the total energy with the required accuracy corresponds to $7 \times 5 \times 9$ k-point grid (96 k-points in IBZ) in both codes.

The results of the As₄Se₄ crystal geometry optimization with different XC functionals and pseudopotentials are presented in Table 1 (cell parameters) along with experimental data and the results of theoretical work (Hasan, Baral, Ching 2019; Hasan 2021), and in Table 2 (atomic positions).

Table 1. Theoretical equilibrium geometry of the As₄Se₄ crystal calculated in the present work by DFT method using CASTEP and Quantum Espresso codes with various XC functionals and pseudopotentials

Code	DFT	Pseudopotentials (type)	Valence electrons	a, b, c (Å)	$\alpha = \gamma; \beta$ (degrees)	Cell volume V_0 (Å ³)	Density (g/cm ³)
CASTEP	PBE+D2 (Grimme)	ONCV	As: 4s ² 4p ³ Se: 4s ² 4p ⁴	9.612 13.811 6.732	90 106.460	857.034	4.770
QE	PBE+D2 (Grimme)	PAW	As: 4s ² 4p ³ Se: 4s ² 4p ⁴	9.617 13.794 6.738	90 106.413	857.396	4.768
QE	PBE+D2 (Grimme)	ONCV	As: 3d ¹⁰ 4s ² 4p ³ Se: 3d ¹⁰ 4s ² 4p ⁴	9.610 13.784 6.734	90 106.424	855.579	4.779
QE	PBEsol+D2 (Grimme)	ONCV	As: 3d ¹⁰ 4s ² 4p ³ Se: 3d ¹⁰ 4s ² 4p ⁴	9.113 13.380 6.518	90 107.173	759.289	5.385
QE	PBEsol	ONCV	As: 3d ¹⁰ 4s ² 4p ³ Se: 3d ¹⁰ 4s ² 4p ⁴	9.267 13.696 6.623	90 107.529	801.529	5.101
CASTEP	PBEsol	ONCV	As: 4s ² 4p ³ Se: 4s ² 4p ⁴	9.281 13.746 6.635	90 107.640	806.712	5.068
VASP (Hasan et al. 2019)	PBE	PAW	As: 4s ² 4p ³ Se: 4s ² 4p ⁴	7.189 14.746 10.580	90 114.840	1121.500	
Expt.				9.63 13.80 6.73	90 107.8	851.562	4.801

Table 2. Fractional coordinates of symmetry non-equivalent atoms in the As₄Se₄ crystal. Experimental data from (Bastow, Whitfield 1973)

	Experimental			PBE+D2 ONCV (CASTEP)			PBE+D2 ONCV (QE)		
	x/a	x/b	x/c	x/a	x/b	x/c	x/a	x/b	x/c
As1	0.1141	0.0182	-0.2452	0.1118	0.0215	-0.2427	0.1114	0.0218	-0.2426
As2	0.4271	-0.1405	-0.1367	0.4297	-0.1369	-0.1355	0.4295	-0.1363	-0.1378
As3	0.3256	-0.1312	0.1752	0.3258	-0.1298	0.1804	0.3258	-0.1301	0.1782
As4	0.0363	-0.1603	-0.2962	0.0366	-0.1604	-0.2993	0.0368	-0.1604	-0.3005
Se1	0.3485	0.0101	-0.3065	0.3466	0.0143	-0.3103	0.3461	0.0153	-0.3107
Se2	0.2132	0.0252	0.1245	0.2131	0.0283	0.1287	0.2127	0.0282	0.1284
Se3	0.2414	-0.2323	-0.3729	0.2449	-0.2324	-0.3731	0.2450	-0.2318	-0.3756
Se4	0.1018	-0.2178	0.0526	0.1016	-0.2189	0.0524	0.1022	-0.2196	0.0503

For the best theoretical equilibrium geometry (row 1 of Table 1), calculated using the CASTEP code with a generalized gradient XC functional in the form of PBE with a vdW correction in the form of Grimme-D2 (Grimme 2006), as well as with ONCV pseudopotentials proposed by Hamann (Hamann 2013) to describe electron-ion interactions, we calculated various electronic structure characteristics reflecting the nature of the chemical bond in As₄Se₄, namely the charge electron density difference (CDD) along with atomic and overlap populations.

In addition, within the framework of the same approach and approximations, we carried out a DFT study of the geometric and electronic structure of the As₄Se₄ crystal versus the As₄Se₄ molecule. Scientific literature contains various theoretical data on the geometry and chemical bonding both in As₄Se₄ molecules and in the As₄Se₄ crystal, but their comparative theoretical analysis in the same approximations is missing. In the present work the geometric structure of the As₄Se₄ molecule was calculated within the periodic model with a cubic box of size 10 × 10 × 10 Å by a plane-wave DFT method with PBE XC functional without vdW correction and with ONCV pseudopotentials.

Charge density difference

The electron density difference (Charge Density Difference, CDD) is defined as the difference in electron density in the structure under study (molecule and crystal) and the sum of isolated atoms. The calculated CDD allows to visualize covalent bonds (CBs) as an increase in electron density between atoms and the lone-pair (LP) electrons, which are associated also with an increased electron density.

Population analysis

Atomic charges in molecules and solids are ill-defined in the sense that they do not represent observable quantities. Therefore, their values should be considered only relative to prototypical systems. Nevertheless, a concept of atomic charge in molecules and crystals is a useful tool because it provides an intuitive way to analyze and interpret the electronic structure. To date, various methods of calculating the atomic and overlap populations have been developed in the quantum chemistry of molecules and solids. The most common and widely used are the Mulliken (Mulliken 1955), Löwdin (Löwdin 1950) and Bader (Bader 1990; Bader et al. 1979) charges. These population analysis schemes are used in the quantum chemistry of solids within both the linear combination of atomic orbitals (LCAO) codes and the plane wave (PW) codes. In the present paper we used the PW implementation of these population analysis schemes (Henkelman et al. 2006; Sanchez-Portal et al. 1995; Sanville et al. 2007; Segall et al. 1996; 2010; Tang et al. 2009).

Results and discussion

Geometric structure of the As₄Se₄ crystal versus the As₄Se₄ molecule

The As₄Se₄ molecule and As₄Se₄ crystal geometric structures are shown in Figs. 1 and 2 respectively. As can be seen from Tables 1 and 2, in the best calculations we performed (the first three rows of Table 1 — calculations with PBE+D2 XC-functionals), the discrepancy between the parameters of the calculated and experimental equilibrium geometry does not exceed 0.2%. In addition, it should be noted that (i) the quality of the equilibrium geometry strongly depends on whether van der Waals corrections are taken into account or not; (ii) in contrast to the PBE+D2, the PBEsol XC functionals, as with and without vdW

correction, do not reproduce well the experimental equilibrium geometry; (iii) the high accuracy of the equilibrium geometry calculated with both ONCV and PAW pseudopotentials indicates the high quality of the pseudopotentials used; and (iv) taking into account the d-electrons of arsenic and sulfur atoms does not affect the quality of the calculated equilibrium geometry.

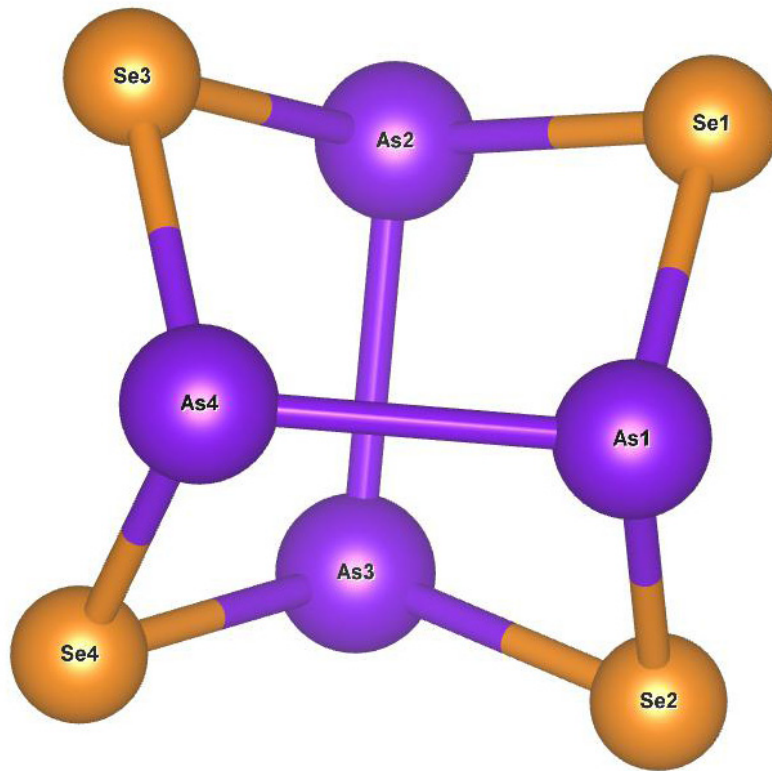


Fig. 1. Structure of the As_4Se_4 molecule. As atoms are shown in violet and Se atoms — in orange

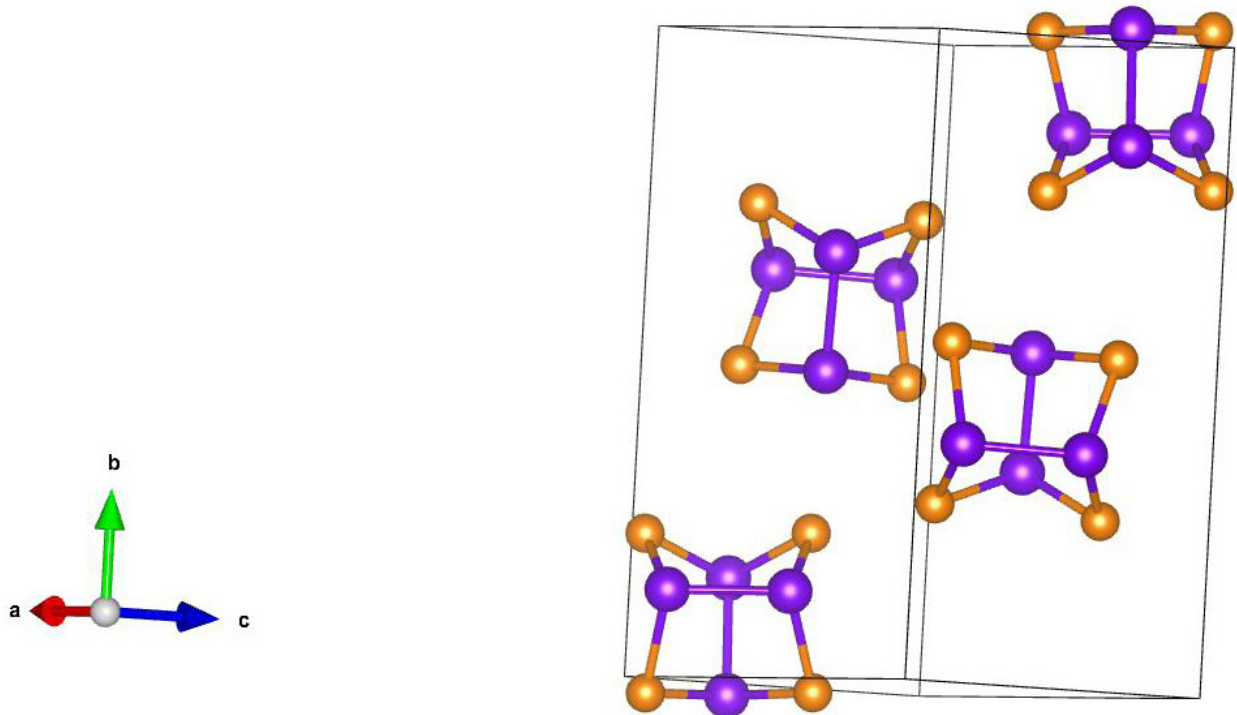


Fig. 2. Structure of the As_4Se_4 crystal. As atoms are shown in violet and Se atoms — in orange

Bond lengths and valence angles in the As₄Se₄ crystal for the best equilibrium geometry and in the As₄Se₄ molecule are presented in Table 3.

Table 3. Bond lengths and angles in the As₄Se₄ crystal versus the molecule calculated by CASTEP (PBE+D2 ONCV for the crystal and PBE ONCV for the molecule) along with experimental data for the As₄Se₄ crystal (Goldstein, Paton 1974)

Bond lengths, Å											
As – As			As – Se				Se – Se				
	Expt	cryst	mol		Expt	cryst	mol		Expt	cryst	mol
As2 – As3	2.560	2.595	2.630	As1 – Se1	2.393	2.428	2.392	Se1 ... Se3	3.487	3.537	3.521
As1 – As4	2.571	2.612	2.630	As2 – Se1	2.385	2.419	2.392	Se3 ... Se4	3.475	3.518	3.521
As2 ... As4	3.591	3.638	3.625	As2 – Se3	2.384	2.417	2.392	Se4 ... Se2	3.511	3.572	3.521
As4 ... As3	3.591	3.639	3.627	As4 – Se3	2.376	2.411	2.392	Se2 ... Se1	3.496	3.545	3.521
As3 ... As1	3.610	3.659	3.627	As4 – Se4	2.378	2.410	2.392				
As1 ... As2	3.610	3.660	3.627	As3 – Se4	2.386	2.418	2.392				
				As3 – Se2	2.387	2.419	2.392				
				As1 – Se2	2.381	2.414	2.392				

Angles, °											
As – Se – As			Se – As – Se				As – As – Se				
	Expt	cryst	mol		Expt	cryst	mol		Expt	cryst	mol
As1 – Se1 – As2	98.2	98.089	98.597	Se1 – As2 – Se3	94.0	94.103	94.776	As4 – As1 – Se2	101.2	101.674	100.719
As2 – Se3 – As4	97.9	97.807	98.541	Se3 – As4 – Se4	93.9	93.724	94.774	As4 – As1 – Se1	100.2	99.587	100.678
As4 – Se4 – As3	97.8	97.824	98.598	Se4 – As3 – Se2	94.7	95.204	94.803	As3 – As2 – Se1	101.9	102.436	100.761
As3 – Se2 – As1	98.4	98.416	98.636	Se2 – As1 – Se1	94.2	94.136	94.802	As3 – As2 – Se3	100.9	100.456	100.778
								As1 – As4 – Se3	102.0	102.438	100.777
								As1 – As4 – Se4	101.6	101.253	100.762
								As2 – As3 – Se4	101.3	101.537	100.677
								As2 – As3 – Se2	100.7	100.192	100.718

As can be seen from Table 3, the As–As bond lengths both in the molecule and the crystal are considerably longer than 2.42 Å, the covalent diameter of the As atom (Schomaker, Stevenson 1941), which qualitatively indicates the presence of effective repulsion between opposite As atoms (As₁–As₄, As₂–As₃). On the other hand, the values of the overlap populations As₁–As₄ and As₂–As₃ (see Table 4) indicate the absence of effective interaction between these atoms in the molecule and its antibonding character between the same atoms in the crystal. This contradicts the generally accepted qualitative ideas about the existence of chemical bonds between the opposite arsenic atoms both in the molecule and in the crystal, although an attempt to describe the complex nature of interactions by considering only pair interactions is very simplified.

Another attempt of this kind of simplified qualitative consideration was made in (Goldstein, Paton 1974). The authors explain the elongation of the As–As bond by a preference of the molecules for a bonding configuration having D_{2d} symmetry concomitant with a minimization of the intramolecular repulsions between non-bonded atoms. In their opinion, evidence of these repulsions is confirmed by the short intramolecular Se...Se separations in As₄Se₄ (see column Expt in Table 3), in contrast to the shortest intra-ring and intra-chain non-bonded Se...Se separations in α-Se (Cherin, Unger 1972) and in trigonal Se (Cherin, Unger 1967) which are equal to 3.72 Å and 3.716 Å respectively.

Table 4. Bond lengths and overlap populations in the As_4Se_4 crystal versus the molecule calculated by CASTEP (PBE+D2 ONCV for the crystal and PBE ONCV for the molecule) along with experimental data for the As_4Se_4 crystal (Goldstein, Paton 1974)

Bond	Bond lengths, Å		Mulliken overlap populations	
	mol	cryst	mol	cryst
As4 – Se4	2.392	2.410	0.24	-0.90
As4 – Se3	2.392	2.410	0.13	-0.41
As1 – Se2	2.392	2.414	0.24	-0.79
As2 – Se3	2.392	2.417	0.13	-0.09
As3 – Se4	2.392	2.418	0.26	-0.06
As2 – Se1	2.392	2.419	0.24	-0.52
As3 – Se2	2.392	2.419	0.24	-0.32
As1 – Se1	2.392	2.428	0.26	-0.15
As2 – As3	2.630	2.595	-0.03	-2.94
As1 – As4	2.630	2.612	-0.03	-2.28

The present DFT calculations demonstrate that the As–Se bond length in the As_4Se_4 molecule is 2.392 Å (see Table 3), which is slightly larger than the sum of the covalent radii of As and Se, 1.21 Å and 1.17 Å respectively (Schomaker, Stevenson 1941), while the average As–Se bond length in the As_4Se_4 crystal was found to be 2.417 Å, which is one percent more than in the molecule. The calculated As–Se bond lengths both for the molecule and the crystal correlate with the sum of the covalent radii of As and Se atoms.

Van der Waals radii of As and Se atoms are 1.85 Å and 1.90 Å respectively following (<https://periodictable.com/Properties/A/VanDerWaalsRadius.v.html>). The DFT calculated distances As–As and Se–Se for atoms belonging to the different molecules of the crystal As_4Se_4 were found to be in agreement with predicted double van der Waals radii of As and Se atoms respectively.

CDD and population analysis for the As_4Se_4 crystal versus the As_4Se_4 molecule

The visualized CDD of the As_4Se_4 molecule and the As_4Se_4 crystal are presented in Figs. 3 and 4 respectively. The CDD clouds reveal an increase in electron density and are marked by red color in the figures. It is generally accepted that CDD clouds indicate the presence of covalent bonds or lone electron pairs. In the case of As_4Se_4 we are talking about bonds As–Se, As–As and lone-pair electrons in regions near As and Se atoms both in the molecule and the crystal. Indeed, being three-fold coordinated, arsenic has a single s^2 lone pair according to valence shell $s^2p_xp_y p_z$ (single red CDD cloud near each As atom). Selenium is two-fold coordinated and has, in addition to a s^2 lone pair, a p_z^2 lone pair according to valence shell $s^2p_xp_y p_z^2$ (two red CDD clouds near each Se atom).

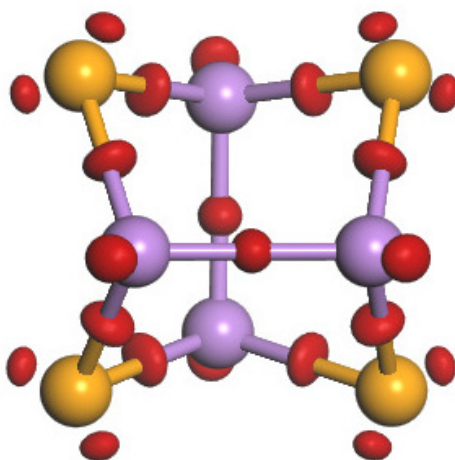


Fig. 3. As_4Se_4 molecule: CDD visualization of the electronic structure

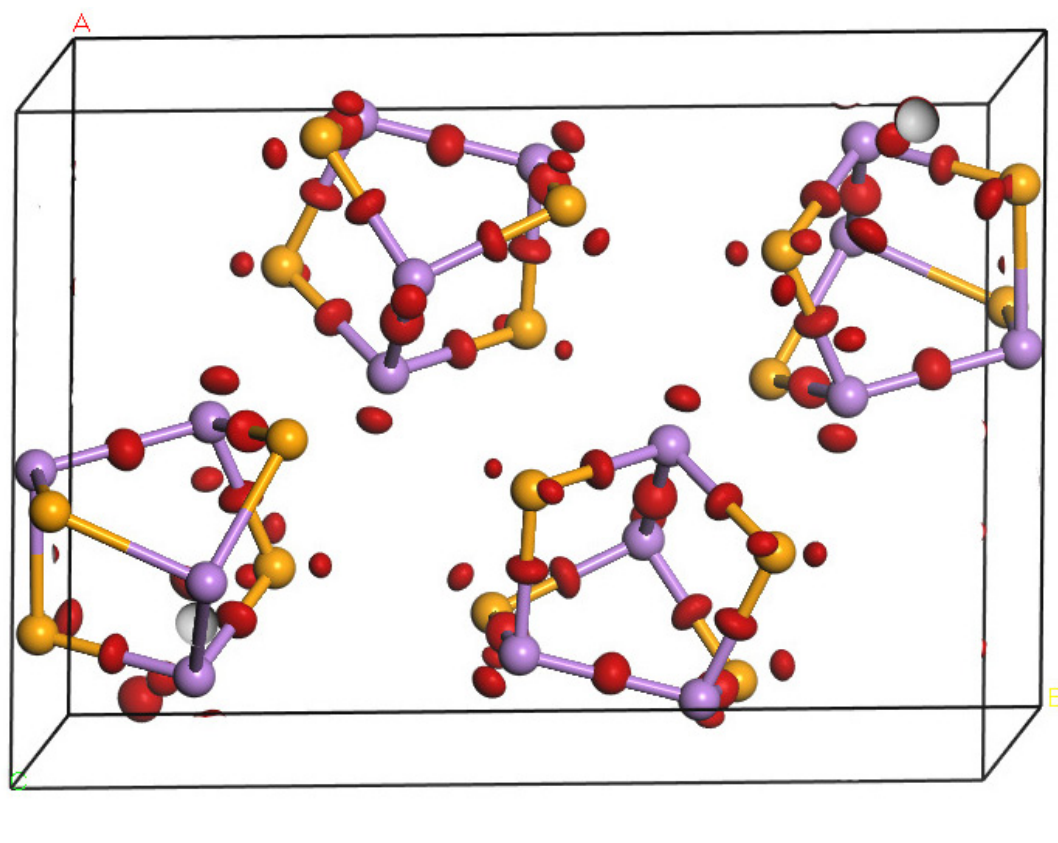


Fig. 4. As₄Se₄ crystal: CDD visualization of the electronic structure

The values of Mulliken, Löwdin and Bader charges in the As₄Se₄ crystal for the best equilibrium geometry along with those in the As₄Se₄ molecule are presented in Table 5. One can see that the absolute values of Mulliken charges for a crystal are on average 20 percent greater than those for a molecule. The values of Bader charges turn out to be almost 2 times greater than the values of the Mulliken and Löwdin charges, which in turn are only slightly different from each other. It is noteworthy that relative differences in the values of the Bader charges for a crystal and a molecule are on average significantly smaller than the corresponding differences for the values of the Mulliken and Löwdin charges, with the exception of atoms As3, As4 and Se2, for which the indicated differences are very significant for all three charge calculation schemes. These significant differences can only be due to intermolecular interactions in the crystal As₄Se₄, which lead to the electron density redistribution. The average Bader charge for As is +0.404 for crystal and +0.409 for molecule, whereas for Se, it is −0.404 and −0.409 respectively. The Bader charges are low, emphasizing only moderate ionic contribution (polar covalency) to the bonding. Overlap populations (Table 4) for the intramolecular As–As distances with lengths 2.595 Å and 2.612 Å are equal to −2.94 and −2.28 respectively. It means the antibonding character of effective interaction between the nearest intramolecular As atoms in the As₄Se₄ crystal. As opposed to the crystal, in the molecule the overlap populations for As–As distances with lengths 2.630 Å are equal to −0.03, which corresponds to the absence of effective interaction between these atoms.

Table 5. Mulliken, Löwdin and Bader charges of the As₄Se₄ crystal

	Mulliken charge		Löwdin charge		Bader charge	
	crystal	molecule	crystal	molecule	crystal	molecule
As1	0.230	0.192	0.195	0.186	0.414	0.410
As2	0.227	0.197	0.179	0.181	0.407	0.405
As3	0.216	0.191	0.198	0.186	0.429	0.411
As4	0.234	0.197	0.155	0.181	0.364	0.410
Se1	−0.207	−0.190	−0.097	−0.087	−0.410	−0.406

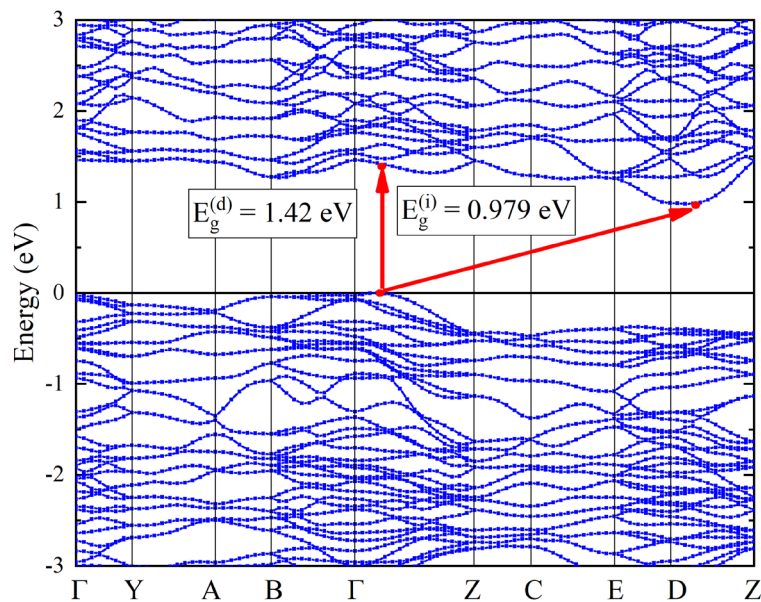
Table 5. Completion

	Mulliken charge		Löwdin charge		Bader charge	
	crystal	molecule	crystal	molecule	crystal	molecule
Se2	-0.214	-0.193	-0.072	-0.084	-0.389	-0.405
Se3	-0.266	-0.203	-0.096	-0.087	-0.409	-0.411
Se4	-0.220	-0.190	-0.103	-0.087	-0.405	-0.415

As₄Se₄ crystal: band structure and DOS

The band structure of the As₄Se₄ crystal calculated by DFT method with PBE XC functional, Grimme-D2 vdW correction and ONCV pseudopotentials, as implemented in CASTEP code, is shown in Fig. 5. It was found that the As₄Se₄ crystal is an indirect gap semiconductor with an indirect gap ($E_g^{(i)}$ in Fig. 5) value of 0.979 eV whereas the direct gap value ($E_g^{(d)}$ in Fig. 5) is 1.42 eV. At the same time, it should be kept in mind that the semilocal XC-functionals usually underestimate the band gap by about 50% due to incomplete exclusion of the electron self-interaction (Perdew, Zunger 1981). The experimental value is expected to be larger, although its magnitude is unknown.

Inspection of the band structure of the As₄Se₄ crystal (Fig. 5) shows that the valence band maximum (VBM) lies in the interval between Γ and Z k-points, while the conduction band minimum (CBM) is in the interval between D and Z k-points, thus forming an indirect band gap. The coordinates of high-symmetry k-points D and Z in Brillouin zone are $(-\frac{1}{2}, 0, \frac{1}{2})$ and $(0, 0, \frac{1}{2})$ respectively.

Fig. 5. Band structure of the As₄Se₄ crystal

In addition to the band structure, we carried out the DFT calculations of the partial densities of states (PDOS) of As and Se atoms in the molecule and the crystal, which are shown in Figs. 6 and 7. In both figures there are two distinct regions in the valence band. The lowest valence band between -15 eV and -8 eV is composed by the s^2 lone pair electron states of As and Se atoms (see also Figs. 3 and 4 for CDD). The highest valence band for the As₄Se₄ crystal lies between -5.5 eV and 0.0 eV (E_F) and exhibits three distinct peaks from p-states of both types of atoms. These three peaks presented in PDOS graphics both of the molecule and the crystal originate from the p_x , p_y and p_z states of As atom and p_x , p_y and p_z^2 states of Se atom. The p_z^2 lone pair of Se atom is clearly visible on the CDD visualization graphs of both the molecule and the crystal (see Figs. 3 and 4). The lone pair nature of p-states near VBM is consistent with widely accepted concepts about electronic structure of chalcogenide materials.

It is worth noting that PDOS structure of the As₄Se₄ crystal calculated in this study is very similar to DOS structure of glassy As₄Se₄ (g-As₄Se₄), calculated in the cluster approach by DFT method (Li, Drabold, Krishnaswami et al. 2002). Although the interpretations of the origin of PDOS three peaks in the

upper valence band of the crystalline and glassy As₄Se₄ differ significantly. So, in the article (Li, Drabold, Krishnaswami et al. 2002) devoted to the g-As₄Se₄, these three peaks are attributed to interactions between various structural elements of the g-As₄Se₄. However, such interpretation seems artificial since the As₄Se₄ crystal does not contain highlighted elements characteristic for g-As₄Se₄, while PDOS structures of the upper valence bands for crystalline and glassy As₄Se₄ consist of the same three peaks.

PDOS of As and Se atoms in the molecule and in the crystal are shown in Figs. 6 and 7. Similar to a crystal, in the case of a molecule, the lowest unoccupied molecular orbital (LUMO) states and the highest occupied molecular orbital (HOMO) states are composed mainly by p-states of As and Se atoms.

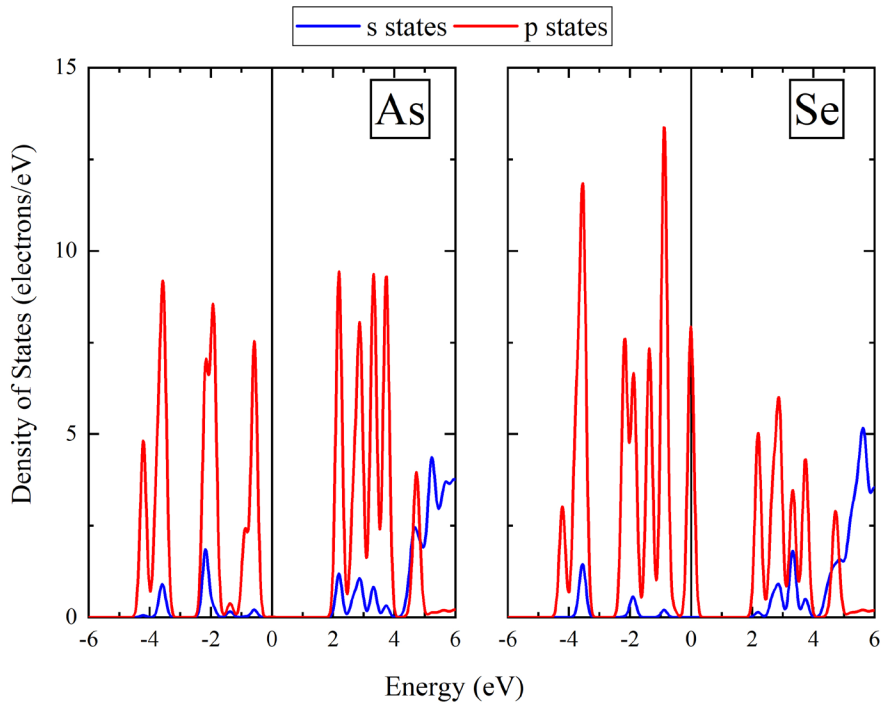


Fig. 6. PDOS for the As₄Se₄ molecule

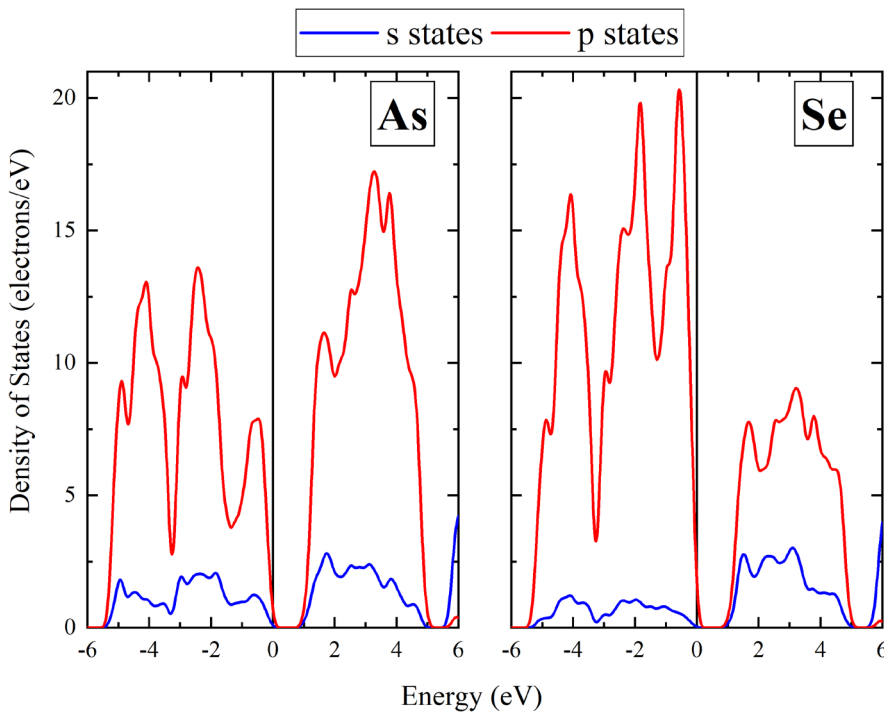


Fig. 7. PDOS for the As₄Se₄ crystal

Conclusions

First, we studied the geometric and electronic structure of the As_4Se_4 crystal versus the As_4Se_4 molecule in the framework of a periodic model by a plane wave DFT method within the same approximations. Equilibrium bond lengths and bond angles were calculated together with charge density differences, Mulliken, Löwdin and Bader charges, and also Mulliken overlap populations, and were compared for the crystal and the molecule. The features of chemical bonding in the As_4Se_4 crystal versus the As_4Se_4 molecule were analyzed. The Bader charges of As and Se atoms turned out to be relatively small both in the molecule and in the crystal, which emphasizes only a moderate ionic contribution to the covalent bond (the so-called polar covalency). A comparative analysis of the overlap populations in the As_4Se_4 molecule and crystal demonstrated the antibonding character of effective interaction between the nearest intramolecular As atoms in the As_4Se_4 crystal and its absence in the molecule. The band structure DFT calculations were carried out and showed that the As_4Se_4 crystal is an indirect-gap semiconductor.

Conflict of Interest

The authors declare that there is no conflict of interest, either existing or potential.

Author Contributions

Conceptualization and methodology — V. G. Kuznetsov; formal analysis, investigation and data curation — V. G. Kuznetsov and A. A. Gavrikov; writing the original draft — A. A. Gavrikov and V. G. Kuznetsov; visualization — A. A. Gavrikov and V. G. Kuznetsov; supervision — V. G. Kuznetsov; discussion of current results and editing — A. A. Gavrikov, V. G. Kuznetsov and V. A. Trepakov.

Acknowledgements

V. G. Kuznetsov and A. A. Gavrikov are grateful to A. V. Kolobov and I. I. Tupitsyn for helpful discussions. Computational resources were provided by the supercomputer facility at Ioffe Institute.

References

- Anderson, P. W. (1969) Localized orbitals for Molecular Quantum Theory. I. The Hückel Theory. *Physical Review*, 181 (1), 25–32. <https://doi.org/10.1103/PhysRev.181.25> (In English)
- Babić, D., Rabii, S. (1988) Self-consistent-field $X\alpha$ scattered-wave calculation of the electronic structure of arsenic chalcogenide molecules. *Physical Review B*, 38 (15), 10490–10498. <https://doi.org/10.1103/PhysRevB.38.10490> (In English)
- Babić, D., Rabii, S., Bernholc, J. (1989) Structural and electronic properties of arsenic chalcogenide molecules. *Physical Review B*, 39 (15), 10831–10838. <https://doi.org/10.1103/PhysRevB.39.10831> (In English)
- Bader, R. F. W. (1990) *Atoms in molecules: A Quantum Theory*. Oxford: Oxford University Press, 438 p. (In English)
- Bader, R. F. W., Anderson, S. G., Duke, A. J. (1979) Quantum topology of molecular charge distributions. 1. *Journal of the American Chemical Society*, 101 (6), 1389–1395. <https://doi.org/10.1021/ja00500a006> (In English)
- Bastow, T. J., Whitfield, H. J. (1973) Crystal structure of tetra-arsenic tetraselenide. *Journal of the Chemical Society, Dalton Transactions*, 17, 1739–1740. <https://doi.org/10.1039/DT9730001739> (In English)
- Beran, G. J. O. (2016) Modeling polymorphic molecular crystals with Electronic Structure Theory. *Chemical Reviews*, 116 (9), 5567–5613. <https://doi.org/10.1021/acs.chemrev.5b00648> (In English)
- Blöchl, P. E. (1994) Projector augmented-wave method. *Physical Review B*, 50 (24), 17953–17979. <https://doi.org/10.1103/PhysRevB.50.17953> (In English)
- Bullett, D. W. (1975) Electronic structures of layer and chain elements by a local orbital method. *The Philosophical Magazine: A Journal of Theoretical Experimental and Applied Physics. Series 8*, 32 (5), 1063–1074. <https://doi.org/10.1080/14786437508221674> (In English)
- Bullett, D. W. (1976a) Electronic structure of arsenic chalcogenides. *Physical Review B*, 14 (4), 1683–1692. <https://doi.org/10.1103/PhysRevB.14.1683> (In English)
- Bullett, D. W. (1976b) Density of states calculation for crystalline As and Sb. *Solid State Communications*, 17 (8), 965–967. [https://doi.org/10.1016/0038-1098\(75\)90230-6](https://doi.org/10.1016/0038-1098(75)90230-6) (In English)
- Chen, I. (1975) Electronic structures of As_4Se_4 and Se_8 . *Physical Review B*, 11 (10), 3976–3982. <https://doi.org/10.1103/PhysRevB.11.3976> (In English)
- Cherin, P., Unger, P. (1967) The crystal structure of trigonal selenium. *Inorganic Chemistry*, 6 (8), 1589–1591. <https://doi.org/10.1021/ic50054a037> (In English)

- Cherin, P., Unger, P. (1972) Refinement of the crystal structure of α -monoclinic Se. *Acta Crystallographica*, B28, 313–317. <https://doi.org/10.1107/S0567740872002249> (In English)
- Clark, S. J., Segall, M. D., Pickard, C. J. et al. (2005) First principles methods using CASTEP. *Zeitschrift für Kristallographie – Crystalline Materials*, 220 (5–6), 567–570. <https://doi.org/10.1524/zkri.220.5.567.65075> (In English)
- Dal Corso, A. (2014) Pseudopotentials periodic table: From H to Pu. *Computational Materials Science*, 95, 337–350. <https://doi.org/10.1016/j.commatsci.2014.07.043> (In English)
- Giannozzi, P., Andreussi, O., Brumme, T. et al. (2017) Advanced capabilities for materials modelling with Quantum ESPRESSO. *Journal of Physics: Condensed Matter*, 29 (46), article 465901. <https://doi.org/10.1088/1361-648X/aa8f79> (In English)
- Giannozzi, P., Baroni, S., Bonini, N. et al. (2009) QUANTUM ESPRESSO: A modular and open-source software project for quantum simulations of materials. *Journal of Physics: Condensed Matter*, 21 (39), article 395502. <https://doi.org/10.1088/0953-8984/21/39/395502> (In English)
- Goldstein, P., Paton, A. (1974) The crystal and molecular structure of tetrameric arsenic selenide, As₄Se₄. *Acta Crystallographica*, B30, 915–920. <https://doi.org/10.1107/S0567740874004043> (In English)
- Grimme, S. (2006) Semiempirical GGA-type density functional constructed with a long-range dispersion correction. *Journal of Computational Chemistry*, 27 (15), 1787–1799. <https://doi.org/10.1002/jcc.20495> (In English)
- Elliott, S. R. (1986) A unified model for reversible photostructural effects in chalcogenide glasses. *Journal of Non-Crystalline Solids*, 81 (1–2), 71–98. [https://doi.org/10.1016/0022-3093\(86\)90260-7](https://doi.org/10.1016/0022-3093(86)90260-7) (In English)
- Elliott, S. R. (1990) *Physics of Amorphous Materials*. London; New York: Longman Publ., 387 p. (In English)
- Eyert, V. (1996) Comparative study on methods for convergence acceleration of iterative vector sequences. *Journal of Computational Physics*, 124 (2), 271–285. <https://doi.org/10.1006/jcph.1996.0059> (In English)
- Hamann, D. R. (2013) Optimized norm-conserving Vanderbilt pseudopotentials. *Physical Review B*, 88 (8), article 085117. <https://doi.org/10.1103/PhysRevB.88.085117> (In English)
- Hasan, S. (2021) *First-principles study of the electronic structure, bonding, optical, mechanical, and thermoelectric properties of bulk chalcogenide crystals*. PhD dissertation (Physics and Mathematics). Kansas, University of Missouri-Kansas City, 213 p. (In English)
- Hasan, S., Baral, K., Ching, W.-Y. (2019) *Total bond order density as a quantum mechanical metric for materials design: Application to chalcogenide crystals*. Preprints, article 2019060199. [Online]. Available at: <https://www.preprints.org/manuscript/201906.0199/v1> (accessed 20.03.2024). (In English)
- Henkelman, G., Arnaldsson, A., Jónsson, H. (2006) A fast and robust algorithm for Bader decomposition of charge density. *Computational Materials Science*, 36 (3), 354–360. <https://doi.org/10.1016/j.commatsci.2005.04.010> (In English).
- Kolobov, A. V. (2003) *Photo-induced metastability in amorphous semiconductors*. Hoboken: Wiley Publ., 412 p. <http://dx.doi.org/10.1002/9783527602544> (In English)
- Kolobov, A. V., Elliott, S. R. (1995) Reversible photo-amorphization of crystalline films of As₅₀Se₅₀. *Journal of Non-Crystalline Solids*, 189 (3), 297–300. [https://doi.org/10.1016/0022-3093\(95\)00245-6](https://doi.org/10.1016/0022-3093(95)00245-6) (In English)
- Krecmer, P., Moulin, A. M., Stephenson, R. J. et al. (1997) Reversible nanocontraction and dilatation in a solid induced by polarized light. *Science*, 277 (5333), 1799–1802. <https://doi.org/10.1126/science.277.5333.1799> (In English)
- Kresse, G., Joubert, D. (1999) From ultrasoft pseudopotentials to the projector augmented-wave method. *Physical Review B*, 59 (3), 1758–1775. <https://doi.org/10.1103/PhysRevB.59.1758> (In English)
- Li, J., Drabold, D. A., Krishnaswami, S. et al. (2002) Electronic Structure of Glassy Chalcogenides As₄Se₄ and As₂Se₃: A Joint Theoretical and Experimental Study. *Physical Review B*, 88 (4), article 046803 <https://doi.org/10.1103/PhysRevLett.88.046803> (In English)
- Löwdin, P.-O. (1950) On the non-orthogonality problem connected with the use of atomic wave functions in the theory of molecules and crystals. *The Journal of Chemical Physics*, 18 (3), 365–375. <https://doi.org/10.1063/1.1747632> (In English)
- Monkhorst, H. J., Pack, J. D. (1976) Special points for Brillouin-zone integrations. *Physical Review B*, 13 (12), 5188–5192. <https://doi.org/10.1103/PhysRevB.13.5188> (In English)
- Mulliken, R. S. (1955) Electronic Population Analysis on LCAO-MO molecular wave functions. I. *The Journal of Chemical Physics*, 23 (10), 1833–1840. <https://doi.org/10.1063%2F1.1740588> (In English)
- Owen, A. E., Firth, A. P., Ewen, P. J. S. (1985) Photo-induced structural and physico-chemical changes in amorphous chalcogenide semiconductors. *Philosophical Magazine Part B*, 52 (3), 347–362. <https://doi.org/10.1080/13642818508240606> (In English)
- Perdew, J. P., Burke, K., Ernzerhof, M. (1996) Generalized gradient approximation made simple. *Physical Review Letters*, 77 (18), 3865–3868. <https://doi.org/10.1103/PhysRevLett.77.3865> (In English)
- Perdew, J. P., Ruzsinszky, A., Csonka, G. I. et al. (2008) Restoring the density-gradient expansion for exchange in solids and surfaces. *Physical Review Letters*, 100 (13), article 136406. <https://doi.org/10.1103/PhysRevLett.100.136406> (In English)
- Perdew, J. P., Zunger, A. (1981) Self-interaction correction to density-functional approximations for many-electron systems. *Physical Review B*, 23 (10), 5048–5079. <https://doi.org/10.1103/PhysRevB.23.5048> (In English).

- Pfrommer, B. G., Côté, M., Louie, S. G., Cohen, M. L. (1997) Relaxation of crystals with the quasi-Newton method. *Journal of Computational Physics*, 131 (1), 233–240. <https://doi.org/10.1006/jcph.1996.5612> (In English)
- Press, W. H., Flannery, B. P., Teukolsky, S. A., Vetterling, W. T. (1992) *Numerical recipes in C: The art of scientific computing*. 2nd ed. Cambridge: Cambridge University Press, 994 p. (In English)
- Renninger, A. L., Averbach, B. L. (1973) Atomic radial distribution functions of As-Se glasses. *Physical Review B*, 8 (4), 1507–1514. <https://doi.org/10.1103/PhysRevB.8.1507> (In English)
- Salaneck, W. R., Liang, K. S., Paton, A., Lipari, N. O. (1975) Electronic structure of molecular arsenic chalcogenides. *Physical Review B*, 12 (2), 725–730 <https://doi.org/10.1103/PhysRevB.12.725> (In English)
- Sanchez-Portal, D., Artacho, E., Soler, J. M. (1995) Projection of plane-wave calculations into atomic orbitals. *Solid State Communications*, 95 (10), 685–690. <https://doi.org/10.1016/0038-1098%2895%2900341-X> (In English)
- Sanville, E., Kenny, S. D., Smith, R., Henkelman, G. (2007) An improved grid-based algorithm for Bader charge allocation. *Journal of Computational Chemistry*, 28 (5), 899–908. <https://doi.org/10.1002/jcc.20575> (In English)
- Schlipf, M., Gygi, F. (2015) Optimization algorithm for the generation of ONCV pseudopotentials. *Computer Physics Communications*, 196, 36–44. <https://doi.org/10.1016/j.cpc.2015.05.011> (In English)
- Schomaker, V., Stevenson, D. P. (1941) Some revisions of the covalent radii and the additivity rule for the lengths of partially ionic single covalent bonds. *Journal of American Chemical Society*, 63 (1), 37–40. <https://doi.org/10.1021/ja01846a007> (In English)
- Segall, M. D., Lindan, P. J. D., Probert, M. J. et al. (2002) First-principles simulation: Ideas, illustrations and the CASTEP code. *Journal of Physics: Condensed Matter*, 14 (11), 2717–2744. <https://doi.org/10.1088/0953-8984/14/11/301> (In English)
- Segall, M. D., Pickard, C. J., Shah, R., Payne, M. C. (2010) Population analysis in plane wave electronic structure calculations. *Molecular Physics: An International Journal at the Interface Between Chemistry and Physics*, 89 (2), 571–577. <http://dx.doi.org/10.1080/002689796173912> (In English)
- Segall, M. D., Shah, R., Pickard, C. J., Payne, M. C. (1996) Population analysis of plane-wave electronic structure calculations of bulk materials. *Physical Review B*, 54 (23), 16317–16320. <https://doi.org/10.1103/PhysRevB.54.16317> (In English)
- Shanno, D. F. (1978) Conjugate gradient methods with inexact searches. *Mathematics of Operations Research*, 3 (3), 244–256. <https://doi.org/10.1287/moor.3.3.244> (In English)
- Shimakawa, K., Yoshida, N., Ganjoo, A. et al. (1998) A model for the photostructural changes in amorphous chalcogenides. *Philosophical Magazine Letters*, 77 (3), 153–158. <http://dx.doi.org/10.1080/095008398178598> (In English)
- Smail, E. J., Sheldrick, G. M. (1974) Tetra-arsenic Tetraselenide. *Acta Crystallographica*, B29, 2014–2016. <https://doi.org/10.1107/S0567740873005972> (In English)
- Tanaka, K. (2001) Chalcogenide Glasses. In: *Encyclopedia of Materials: Science and Technology*. 2nd ed. Oxford: Elsevier Publ., pp. 1123–1131. <https://doi.org/10.1016/B0-08-043152-6/00210-2> (In English)
- Tanaka, K., Yamabe, T., Tachibana, A. et al. (1978) Electronic structures of tetrasulfur tetranitride, tetraarsenic tetrasulfide, and tetraarsenic tetraselenide, and their anionic species. *Journal of Physical Chemistry*, 82 (19), 2121–2126. <https://doi.org/10.1021/j100508a013> (In English)
- Tang, W., Sanville, E., Henkelman, G. (2009) A grid-based Bader analysis algorithm without lattice bias. *Journal of Physics: Condensed Matter*, 21 (8), article 084204. <http://dx.doi.org/10.1088/0953-8984/21/8/084204> (In English)
- Van Setten, M. J., Giantomassi, M., Bousquet, E. et al. (2018) The PseudoDojo: Training and grading a 85 element optimized norm-conserving pseudopotential table. *Computer Physics Communications*, 226, 39–54. <https://doi.org/10.1016/j.cpc.2018.01.012> (In English)
- Yang, C. Y., Paesler, M. A., Sayers, D. E. (1987) Measurement of local structural configurations associated with reversible photostructural changes in arsenic trisulfide films. *Physical Review B*, 36 (17), 9160–9167. <https://doi.org/10.1103/PhysRevB.36.9160> (In English)